LEGIBILITY NOTICE

A major purpose of the Technical Information Center is to provide the broadest dissemination possible of information contained in DOE's Research and Development Reports to business, industry, the academic community, and federal, state and local governments.

Although a small portion of this report is not reproducible, it is being made available to expedite the availability of information on the research discussed herein.

LA-UR -88-3182

Los Alamos National Laboratory is operated by the University of California for the United States Department of Energy under contract W-7405 ENG-36

LA-UR--88-3182

DE89 000315

TITLE RADIOGRAPHIC STUDIES AND HYDROCODE SIMULATIONS OF TWO TANTALUM EFPs

AUTHOR(S) J. A. SCHWALBE

SUBMITTED TO Workshop on Tantalum for Aerostable EFPs
October 18-19, 1988
Picatinny Arsenal, NJ

Los Alamos National Laboratory
Los Alamos, New Mexico 87545

RADIOGRAPHIC STUDIES AND HYDROCODE SIMULATIONS OF TWO TANTALUM EFPs

L. A. SCHWALBE

Los Alamos National Laboratory
Los Alamos, New Mexico 87545

The Army Research Development and Engineering Center (ARDEC) commissioned Los Alamos to provide Honeywell, Inc. with one high-energy flash radiograph for each of two explosively formed penetrators (EFPs) of tantalum. The two axi-symmetric warheads were identical in their basic design, but their liner contours were different. The first shot, which we designate as H853, used Honeywell's liner design #1; the second shot, H854, used design #2.

The experiments were planned and directed by J. M. Christian (M-4) and were performed at the Ector radiographic facility (R-306) during the week of February 22, 1988. Data reduction and analyses were accomplished over the next several months by K. H. Mueller, Jr. (M-4) and L. A. Schwalbe (X-3). In addition to the experimental work, the computations group (X-3) offered to run hydrodynamic code simulations of the EFP formation for the two designs. Some of the results and conclusions of this theoretical work are also presented below.

EXPERIMENTAL

Shots H853 and H854 follow earlier work at Los Alamos on both copper [1] and tantalum [2] EFPs, but the present experiments were somewhat less complicated because only radiographic data were required. The primary questions at issue concerned the mass distributions: Honeywell expressed particular interest in determining the center of mass coordinates of each penetrator. To get this information, we tailored the x ray source to produce a beam with the highest practical effective mean energy, 1.4 ± 0.1 MeV [2]. In each experiment, the

radiographic exposures were made 745 μs after the loadring signal, to reveal an image of the fully formed penetrator in flight about 1.65 m downrange from the position of the unfired liner. The radiographic film pack consisted of six stacked and registered films, four Dupont NDT-75 (N) and two Kodak SO-142 (KK), interleaved with 10-mil (254-μm-thick) lead image intensifying screens. Images of both the dynamic EFP and the static step wedge on each film were then digitized at 300-μm pixel intervals and combined using the weighted averaging technique developed by Whitman [3].

The composite image of the EFP from shot H853 is shown in Fig. 2. We could not obtain precise values for the total mass of either this penetrator or the one produced from the second shot. To do this satisfactorily requires an accurate estimate of the spatially varying background density produced on the film by scattered radiation. In some situations this is possible, but here, the irregular geometries of the EFPs and nonuniformities in the static step wedge data produced large uncertainties in the background models.

Unlike the estimates for the total mass, we found those for the CM coordinates to be quite insensitive to the assumed background. We calculated CM positions with a range of constant background values and found the resulting locations varying by only a few pixels. The CM, indicated by the white cross in Fig. 2, is located slightly below the long axis of the penetrator, and its distance behind the leading edge is about 57% of the total length.

Besides CM locations, we produced tomographic reconstructions of the axisymmetric nose sections of each EFP. Figure 3 shows the results for H853. The radiographic image of the nose is reproduced above, and the corresponding tomographic reconstruction appears below. Of particular interest in this figure is the angular structure of the inner contour, a feature we had not observed in earlier data [1,2]. Evidently, in the process of rearward fold-

ing, liner #1 produces two circumferential buckling points. The irregularities at the left of the reconstructed image are caused by deviations from axisymmetry. The apparent sharp boundary within the material in the nose of the EFP is an artifact from the film combination process.

The composite radiographic image from shot H854 is shown in Fig. 4. Here again, the CM position is indicated by the white cross. The EFP of H854 has its CM position 55% of the length behind the nose. Figure 5 shows the enlarged radiographic image and tomographic reconstruction of the EFP nose from H854. Once again, we observe evidence for buckling in the formation process, but, in this case, only a single circumferential buckling point is evident. The inner contour therefore appears blunted or squared-off. On the outside contour of the leading edge of the nose, a small indentation appears slightly below center. The indentation is visible in both the radiograph and the reconstruction, and we speculate that it may have been formed either from spallation off the front surface or from severe localized material flow in this region.

THEORETICAL

Calculations of the EFP formations were run with PINON, a 2D Eularian code with an interface reconstruction feature. For each of the EFP calculations, we used a constant, 1-mm-square mesh. A tabulated equation of state (EOS) was used for the tantalum liner, and the standard JWL parameters [4] were taken for the LX-14 high explosive (HE). For the problems discussed below, we used an ideal-gas EOS (with $\gamma = 5/3$ and $\rho = 0.1$ gm/cc) for the foam in front of the liner (see Fig. 1). Results with this model were identical to those obtained in test cases where a tabulated EOS was used for an initially underdense plastic material that was subsequently crushed up.

The purpose of running the simulations was to see how the results would be affected by changes in the strength model for the tantalum. For most of the work, we used the simple elastic-perfectly plastic strength model and studied the effects of varying the yield strength Y_0. Figure 6 shows some results for the warhead design of H853. The plots are of the material contours of an axial cross section of the penetrator. All three simulations correctly predict the general features of the radiograph of Fig. 2—for example, the hollow, rounded nose and the flared aft sections. But the degree of collapse shown in the computed result with Y_0 = 6.3 kbar most nearly matches that observed experimentally.

The results of similar calculations with the warhead design of H854 are shown in Fig. 7. Here again, within the context of a 2D model that cannot produce the folding structures visible in the radiographic image of the tail, the general features of the experimental data are reproduced adequately. As we noted in the calculations for H853, the radial collapse predicted for the EFP of H854 by the elastic-plastic model with Y_0 = 6.3 kbar best matches the experimental result of Fig. 4.

Ultimately, the elastic-plastic model is a fairly crude approximation to the actual strength properties of the material, and we had hoped to improve our calculations by using the more sophisticated Jonnson-Cook model [5], which incorporates the effects of temperature, material strain and strain-rate. However, we found these simulations to be rather disappointing. In general, the results with thermal softening predict yield strengths to be much too low. To illustrate this, we show at the top of Fig. 8 a material contour plot for the H853 penetrator at 200 μs after the HE initiation. The EFP has collapsed almost completely leaving a residual internal cavity at the forward end and jetting material out the rear.

We suspected that our modelling of thermal softening may have been too severe. Our preliminary calculations with the elastic-plastic model predicted material temperatures for the EFPs in the range from 700 to 950°C, which would lead to 60 to 70% reductions in Y_o with our assumed Johnson-Cook parameters. To see the effect of neglecting thermal softening in Y_o, we reran our two problems using only the strain and strain-rate dependent factors in the standard form [5]. These calculations gave EFPs that were relatively too stiff. The bottom of Fig. 8 shows a typical result. The EFP contours obtained with the above Johnson-Cook parameters without thermal softening most nearly resemble the ones we were seeing with the simple elastic-plastic model for Y_o = 7.7 kbar or higher. We conclude that some adjustments are necessary to adequately model tantalum strength with PINON.

REFERENCES

1. J. M. Christian, K. H. Mueller, Jr., L. A. Schwalbe, V. Draxler, and F. Williamson, "High-Energy Flash Radiography of Two Axisymmetric Copper Explosively Formed Penetrators," International Advances in Nondestructive Testing 13, 361-391 (1988).

2. L. A. Schwalbe, K. H. Mueller, Jr., J. M. Christian, and P. J. DiBona, "In-Flight Radiographic Study of Two Nonaxisymmetric, Explosively Formed Penetrators," LA--Series report LA-11131, Los Alamos National Laboratory, Los Alamos, NM 87545 (March 1988).

3. R. L Whitman, "Combination of Several Radiographic Film Types," manuscript in preparation.

4. B. M. Dobratz and P. C. Crawford, LLNL Explosives Handbook, Lawrence Livermore National Laboratory Report UCRL-52997 Change 2, Jan. 31, 1985.

5. G. R. Johnson and W. H. Cook, "A Constitutive Model and Data for Metals Subjected to Large Strains, High Strain Rates, and High Temperatures," Seventh International Symposium on Ballistics, The Hague, The Netherlands, (April 1983).

FIGURE CAPTIONS

Figure 1. Deleted

Figure 2. Composite radiographic image of the EFP from shot H853. The CM location is shown by the white cross. Corners of the area reproduced at the top of Fig. 3 are indicated here by the dark right angles.

Figure 3. Radiographic image of the EFP nose section from H853 (above) and the tomographic reconstruction of the same area (below).

Figure 4. Composite radiographic image of the EFP from shot H854. The CM location is shown by the white cross. Corners of the area reproduced at the top of Fig. 5 are indicated here by the dark right angles.

Figure 5. Radiographic image of the EFP nose section from H854 (above) and the tomographic reconstruction of the same area (below).

Figure 6. Material contours predicted for the EFP of H853 by PINON at 745 μs after HE detonation. All calculations used an elastic-plastic strength model with the yield stresses indicated.

Figure 7. Material contours predicted for the EFP of H854 by PINON at 745 μs after HE detonation. All calculations used an elastic-plastic strength model with the yield stresses indicated.

Figure 8. Material contours predicted for the EFP of H853 by PINON. Above are the results after 200 μs using the Johnson-Cook strength model with thermal softening; below are the results for the same problem at 745 μs without thermal softening.

Figure 1

deleted.

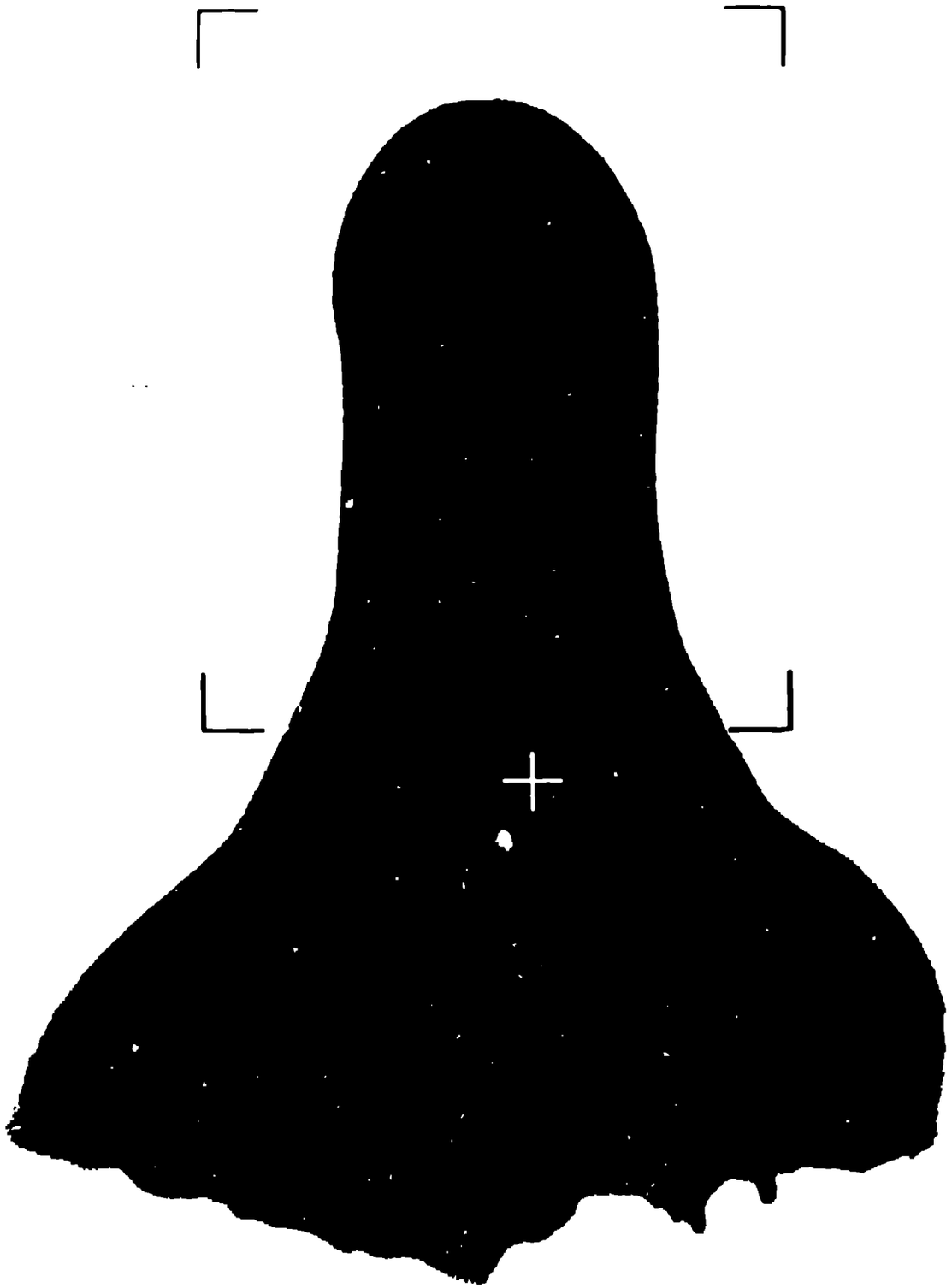

FIGURE 2

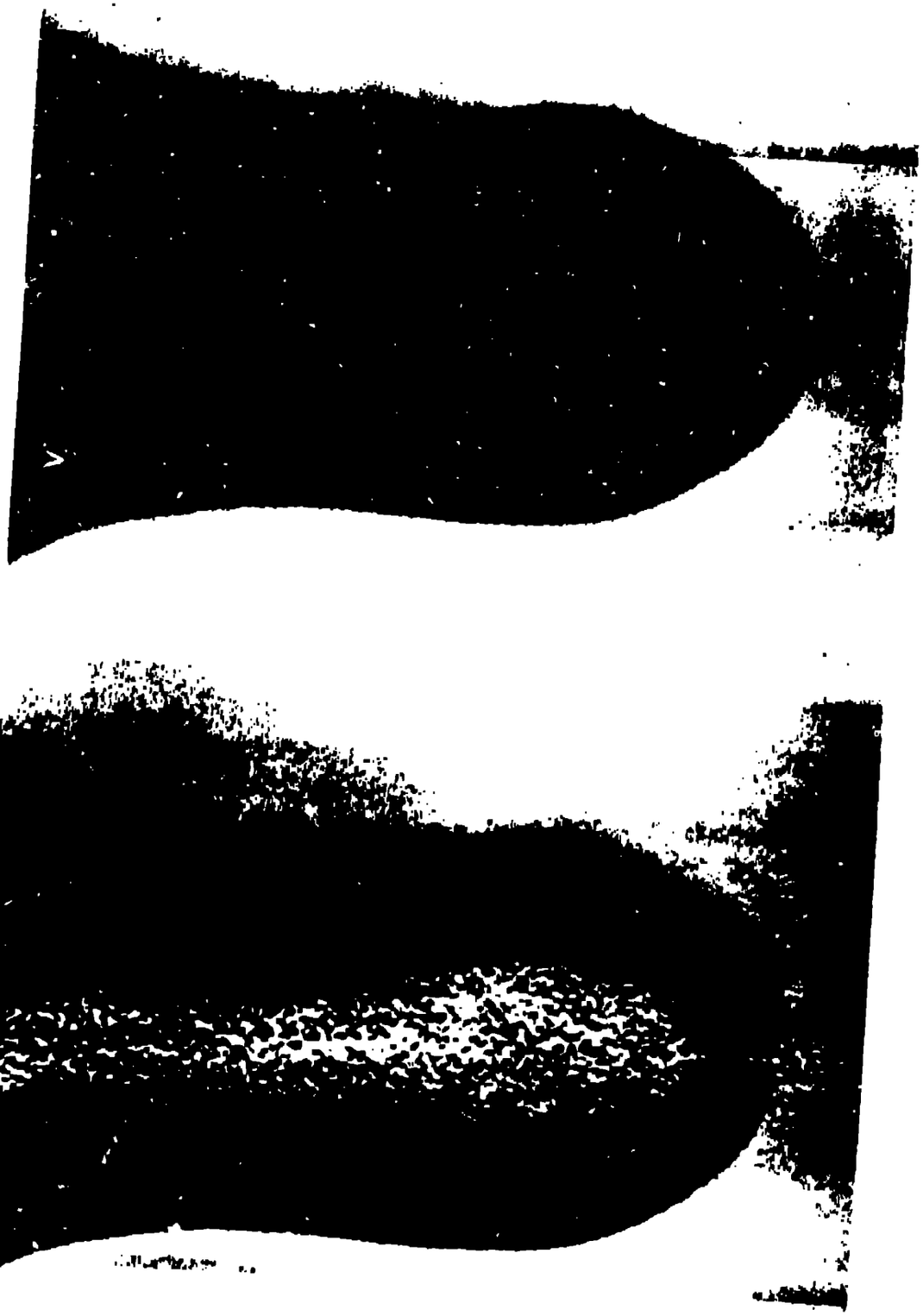

FIGURE 3

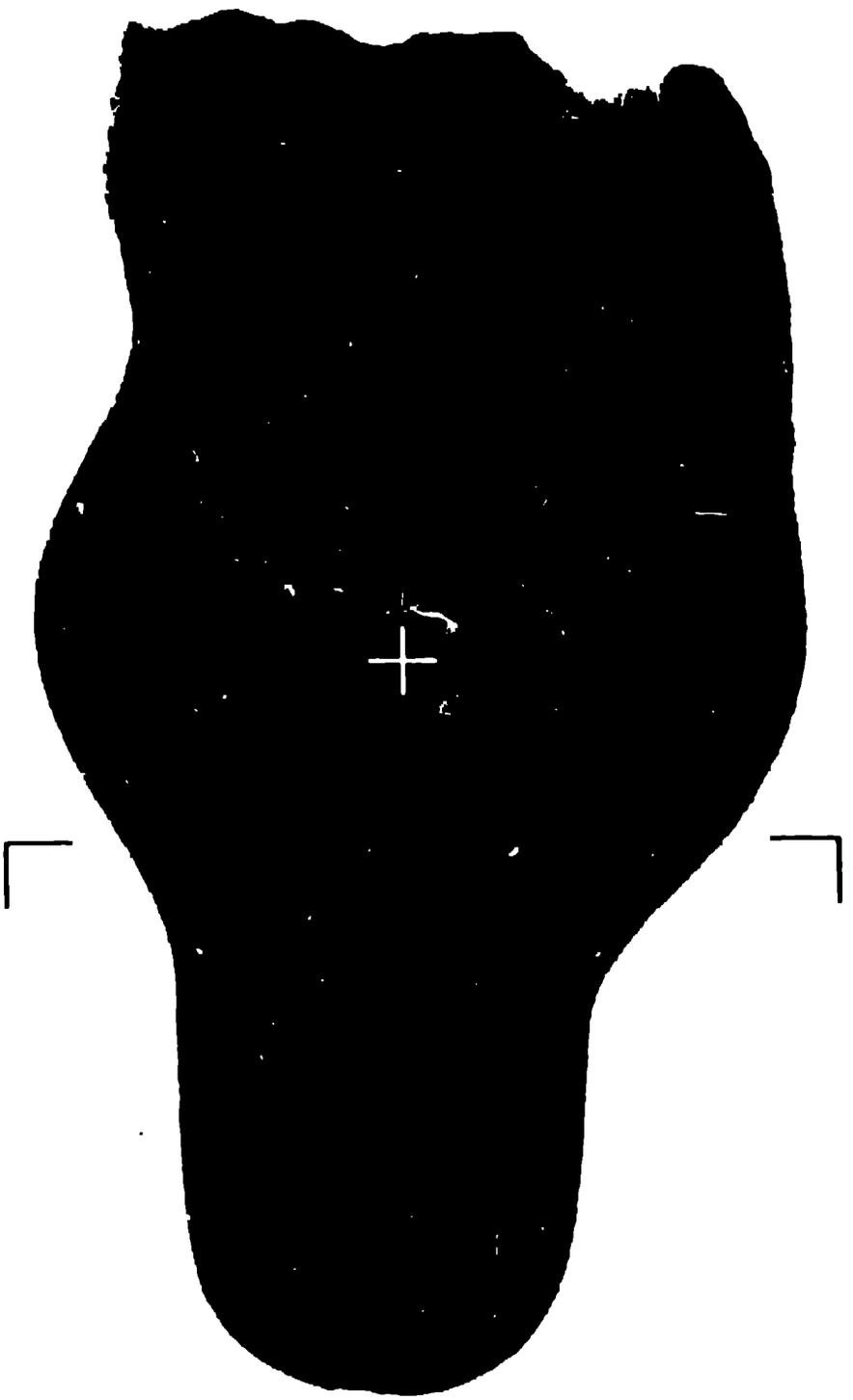

FIGURE 4

FIGURE 5

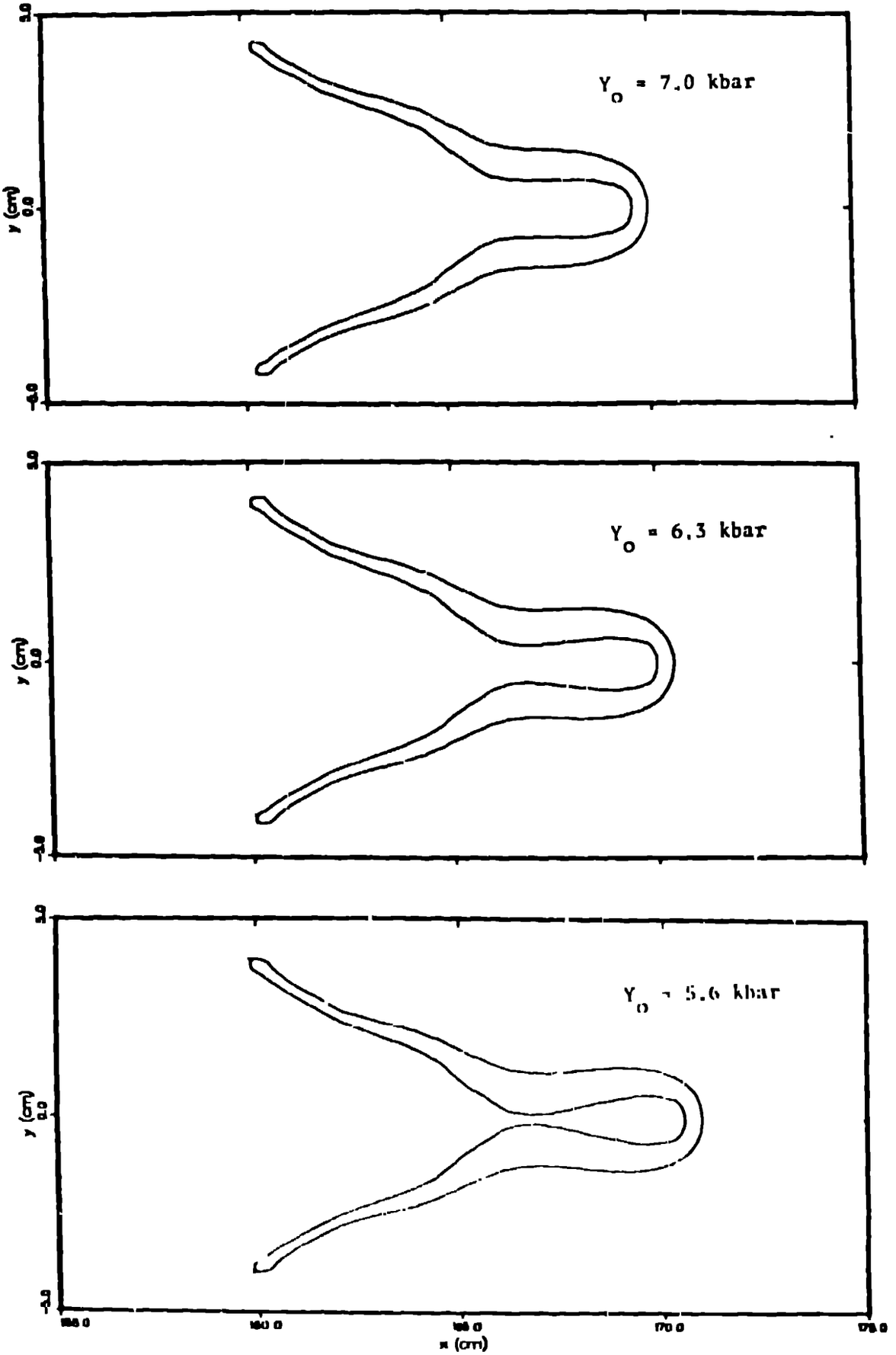

FIGURE 6

H854 -- Honeywell Ta EFP Liner [redacted] 3FC

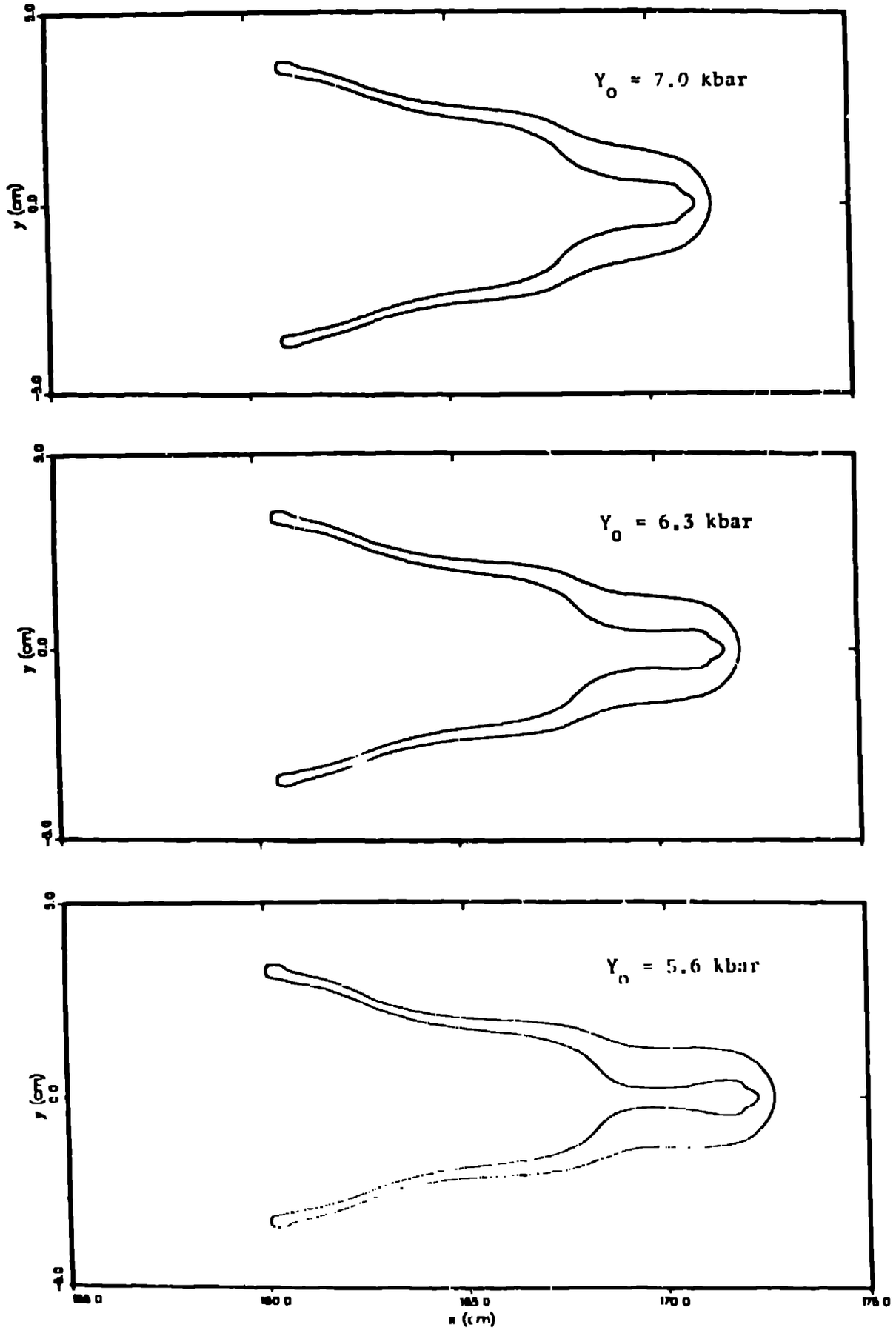

FIGURE 7

H853 -- PINON Simulation with Johnson-Cook Model

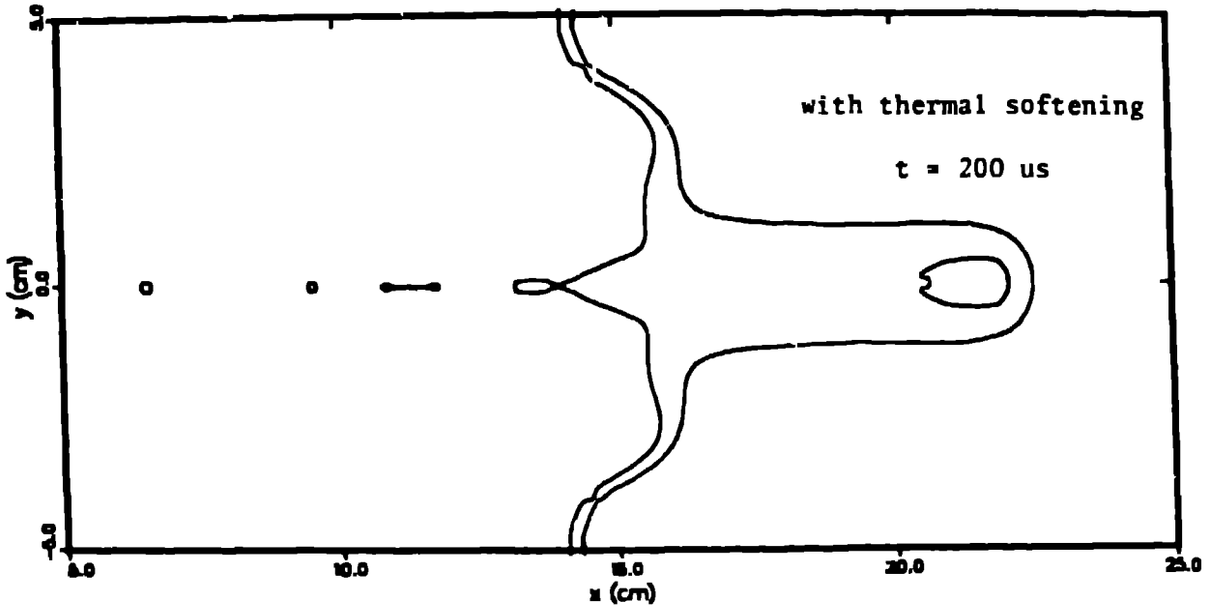

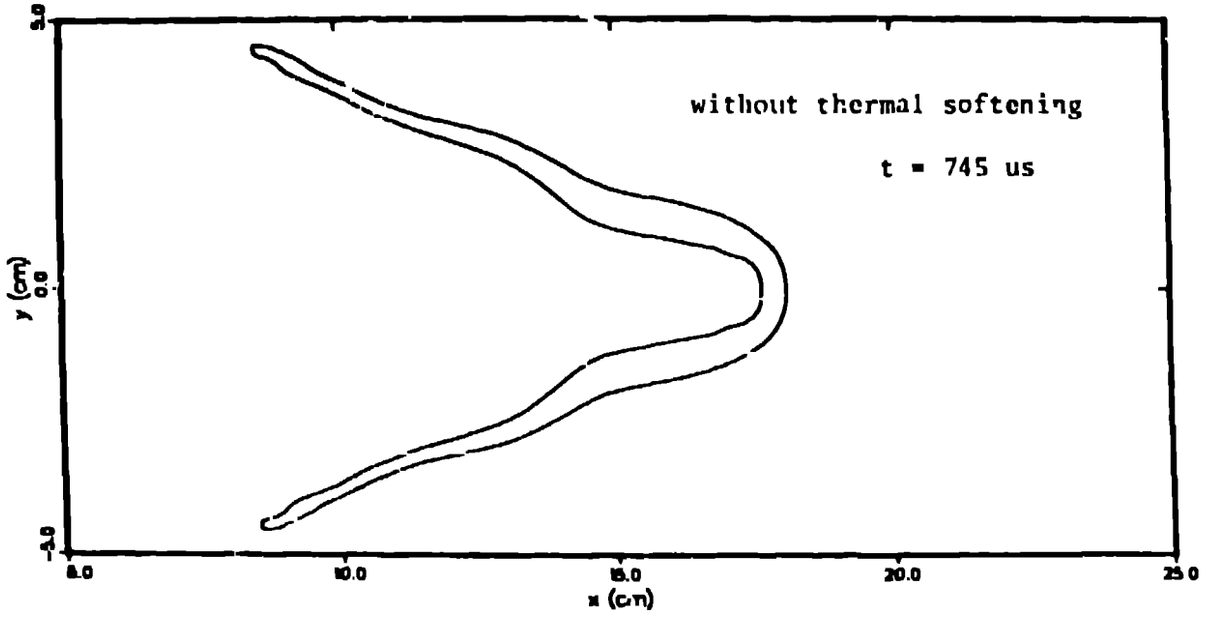

FIGURE 8